# Equation of state of atomic systems beyond $s$-wave determined by the lowest order constrained variational method: Large scattering length limit

Ryan M. Kalas[(1)] and D. Blume[(1,2)]
[(1)] *Department of Physics and Astronomy, Washington State University, Pullman, Washington 99164-2814*
[(2)] *INFM-BEC, Dipartimento di Fisica, Università di Trento, I-38050 Povo, Italy*

Dilute Fermi systems with large $s$-wave scattering length $a_s$ exhibit universal properties if the interparticle spacing $r_o$ greatly exceeds the range of the underlying two-body interaction potential. In this regime, $r_o$ is the only relevant length scale and observables such as the energy per particle depend only on $r_o$ (or, equivalently, the energy $E_{FG}$ of the free Fermi gas). This paper investigates Bose and Fermi systems with non-vanishing angular momentum $l$ using the lowest order constrained variational method. We focus on the regime where the generalized scattering length becomes large and determine the relevant length scales. For Bose gases with large generalized scattering lengths, we obtain simple expressions for the energy per particle in terms of a $l$-dependent length scale $\xi_l$, which depends on the range of the underlying two-body potential and the average interparticle spacing. We discuss possible implications for dilute two-component Fermi systems with finite $l$. Furthermore, we determine the equation of state of liquid and gaseous bosonic helium.

PACS numbers:

## I. INTRODUCTION

The experimental realization of dilute degenerate Bose and Fermi gases has led to an explosion of activities in the field of cold atom gases. A particularly intriguing feature of atomic Bose and Fermi gases is that their interaction strengths can be tuned experimentally through the application of an external magnetic field in the vicinity of a Feshbach resonance [1, 2]. This external knob allows dilute systems with essentially any interaction strength, including infinitely strongly attractive and repulsive interactions, to be realized. Feshbach resonances have been experimentally observed for $s$-, $p$- and $d$-wave interacting gases [3, 4, 5, 6, 7] and have been predicted to exist also for higher partial waves.

A Feshbach resonance arises due to the coupling of two Born-Oppenheimer potential curves coupled through a hyperfine Hamiltonian, and requires, in general, a multichannel description. For $s$-wave interacting systems, Feshbach resonances can be classified as broad or narrow [8]. Whether a resonance is broad or narrow depends on whether the energy width of the resonance is large or small compared to the characteristic energy scale, such as the Fermi energy or the harmonic oscillator energy, of the system. In contrast to $s$-wave resonances, higher partial wave resonances are necessarily narrow due to the presence of the angular momentum barrier [9]. This paper uses an effective single channel description to investigate the behaviors of strongly-interacting Bose and Fermi systems with different orbital angular momenta.

In dilute homogeneous Bose and Fermi gases with large $s$-wave scattering length $a_s$, a regime has been identified in which the energy per particle takes on a universal value which is set by a single length scale, the average interparticle spacing $r_o$ [10, 11, 12]. In this so-called unitary regime, the length scales of the $s$-wave interacting system separate according to $|a_s| \gg r_o \gg R$, where $R$ denotes the range of the two-body potential. The energy per particle $E_{B,0}/N$ (the subscripts "$B$" and "0" stand respectively for "boson" and "$s$-wave interacting") for a homogeneous one-component gas of bosons with mass $m$ in the unitary regime has been calculated to be $E_{B,0}/N \approx 13.3\,\hbar^2 n_B^{2/3}/m$ using the lowest order constrained variational (LOCV) method [12]. The energy $E_{B,0}/N$ at unitarity is thus independent of $a_s$ and $R$, and depends on the single length scale $r_o$ through the boson number density $n_B$, $r_o = (4\pi n_B/3)^{-1/3}$. However, Bose gases in the large scattering length limit are expected to be unstable due to three-body recombination [13, 14, 15, 16].

On the other hand, the Fermi pressure prevents the collapse of two-component Fermi gases with equal masses and equal number of "spin-up" and "spin-down" fermions with large interspecies $s$-wave scattering length [10, 11, 17, 18]. At unitarity, the energy per particle is given by $E_{F,0}/N \approx 0.42 E_{FG}$, where $E_{FG} = (3/10)(\hbar^2 k_F^2/m)$ denotes the energy per particle of the non-interacting Fermi gas [19, 20, 21, 22]. The Fermi wave vector $k_F$ is related to the number density of the Fermi gas by $n_F = k_F^3/3\pi^2$, which implies that $E_{F,0}/N$ depends on $r_o$ but is independent of $a_s$ and $R$. We note that the inequality $|a_s| \gg r_o$ is equivalent to $1/(k_F|a_s|) \ll 1$.

This paper investigates Bose and Fermi systems with large generalized scattering lengths using the LOCV method. For $p$- and $d$-wave interacting Bose systems, we define the unitary regime [23] through the inequalities $|a_l(E_{rel})| \gg \xi_l \gg R$, where $\xi_l$ denotes a $l$-dependent length scale given by the geometric combination of $r_o$ and $R$, i.e., $\xi_l = r_o^{(1-l/4)} R^{l/4}$, and $E_{rel}$ the relative scattering energy. The generalized energy-dependent scattering length $a_l(E_{rel})$ [24, 25, 26] characterizes the scattering strength (see below). We find that the energy of $p$-wave interacting two-component Bose gases and $d$-wave interacting one- and two-component Bose gases at unitary is determined by the combined length $\xi_l$. While Bose gases with higher angular momentum in the unitary regime are

of theoretical interest, they are, like their $s$-wave cousin, expected to be unstable. We comment that the energetics of two-component Fermi gases with large generalized scattering length may depend on the same length scales.

Furthermore, we consider $s$-wave interacting Bose systems over a wide range of densities. Motivated by two recent studies by Gao [27, 28], we determine the energy per particle $E_{B,0}/N$ of the Bose system characterized by two atomic physics parameters, the $s$-wave scattering lengh $a_s$ and the van der Waals coefficient $C_6$. Our results lead to a phase diagram of liquid helium in the low-density regime that differs from that proposed in Ref. [28].

Section II describes the systems under study and introduces the LOCV method. Section III describes our results for dilute $s$-wave interacting Bose and Fermi systems and for liquid helium. Section IV considers Bose and Fermi systems interacting through $l$-wave ($l > 0$) scattering. Finally, Section V concludes.

## II. LOCV METHOD FOR BOSONS AND FERMIONS

This section introduces the three-dimensional Bose and Fermi systems under study and reviews the LOCV method [29, 30, 31, 32]. The idea of the LOCV method is to explicitly treat two-body correlations, but to neglect three- and higher-body correlations. This allows the many-body problem to be reduced to solving an effective two-body equation with properly chosen constraints. Imposing these constraints makes the method non-variational, i.e., the resulting energy does not place an upper bound on the many-body energy. The LOCV method is expected to capture some of the key physics of dilute Bose and Fermi systems.

The Hamiltonian $H_B$ for a homogeneous system consisting of identical mass $m$ bosons is given by

$$H_B = -\frac{\hbar^2}{2m}\sum_i \nabla_i^2 + \sum_{i<j} v(r_{ij}), \qquad (1)$$

where the spherically symmetric interaction potential $v$ depends on the relative distance $r_{ij}$, $r_{ij} = |\mathbf{r}_i - \mathbf{r}_j|$. Here, $\mathbf{r}_i$ denotes the position vector of the $i$th boson. The Hamiltonian $H_F$ for a two-component Fermi system with equal masses and identical spin population is given by

$$H_F = -\frac{\hbar^2}{2m}\sum_i \nabla_i^2 - \frac{\hbar^2}{2m}\sum_{i'} \nabla_{i'}^2 + \sum_{i,i'} v(r_{ii'}), \qquad (2)$$

where the unprimed subscripts label spin-up and the primed subscripts spin-down fermions. Throughout, we take like fermions to be non-interacting. Our primary interest in this paper is in the description of systems for which many-body observables are insensitive to the short-range behavior of the atom-atom potential $v(r)$. This motivates us to consider two simple model potentials: an attractive square well potential $v_{sw}$ with depth $V_o$ ($V_o \geq 0$),

$$v_{sw}(r) = \begin{cases} -V_o & \text{for} \quad r < R \\ 0 & \text{for} \quad r > R\,; \end{cases} \qquad (3)$$

and an attractive van der Waals potential $v_{vdw}$ with hardcore $r_c$,

$$v_{vdw}(r) = \begin{cases} \infty & \text{for} \quad r < r_c \\ -C_6/r^6 & \text{for} \quad r > r_c\,. \end{cases} \qquad (4)$$

In all applications, we choose the hardcore $r_c$ so that the inequality $r_c \ll \beta_6$, where $\beta_6 = (mC_6/\hbar^2)^{1/4}$, is satisfied. The natural length scale of the square well potential is given by the range $R$ and that of the van der Waals potential by the van der Waals length $\beta_6$. The solutions to the two-body Schrödinger equation for $v_{sw}$ are given in terms of spherical Bessel and Neumann functions (imposing the proper continuity conditions of the wave function and its derivations at those $r$ values where the potential exhibits a discontinuity), and those for $v_{vdw}$ in terms of convergent infinite series of spherical Bessel and Neumann functions [33].

The interaction strength of the short-range square well potential can be characterized by the generalized energy-dependent scattering lengths $a_l(k)$,

$$a_l(k) = \mathrm{sgn}[-\tan\delta_l(k)] \left| \frac{\tan\delta_l(k)}{k^{2l+1}} \right|^{1/(2l+1)}, \qquad (5)$$

where $\delta_l(k)$ denotes the phase shift of the $l$th partial wave calculated at the relative scattering energy $E_{rel}$, $k = \sqrt{mE_{rel}/\hbar^2}$. This definition ensures that $a_l(k)$ approaches a constant as $k \to 0$ [34, 35]. For the van der Waals potential $v_{vdw}$, the threshold behavior changes for higher partial waves and the definition of $a_l(k)$ has to be modified accordingly [34, 35]. In general, for a potential that falls off as $-r^{-n}$ at large interparticle distances, $a_l(k)$ is defined by Eq. (5) if $2l < n-3$ and by

$$a_l(k) = \mathrm{sgn}[-\tan\delta_l(k)] \left| \frac{\tan\delta_l(k)}{k^{n-2}} \right|^{1/(n-2)} \qquad (6)$$

if $2l > n-3$. For our van der Waals potential, $n$ is equal to 6 and $a_l(k)$ is given by Eq. (5) for $l \leq 1$ and by Eq. (6) for $l \geq 2$. The zero-energy generalized scattering lengths $a_l$ can now be defined readily through

$$a_l = \lim_{k\to 0} a_l(k). \qquad (7)$$

We note that a new two-body $l$-wave bound state appears at threshold when $|a_l| \to \infty$. The unitary regime for higher partial waves discussed in Sec. IV is thus, as in the $s$-wave case, closely related to the physics of extremely weakly-bound atom-pairs. To uncover the key behaviors at unitarity, we assume in the following that the many-body system under study is interacting through a single partial wave $l$. While this may not be exactly realized in an experiment, this situation may be approximated by utilizing Feshbach resonances.

We now outline how the energy per particle $E_{B,l}/N$ of a one-component Bose system with $l$-wave interactions [36] is calculated by the LOCV method [29, 30, 31, 32]. The boson wave function $\Psi_B$ is taken to be a product of pair functions $f_l$,

$$\Psi_B(\mathbf{r}_1,\ldots,\mathbf{r}_N)=\prod_{i<j} f_l(r_{ij}), \tag{8}$$

and the energy expectation value of $H_B$, Eq. (1), is calculated using $\Psi_B$. If terms depending on the coordinates of three or more different particles are neglected, the resulting energy is given by the two-body term in the cluster expansion,

$$\frac{E_{B,l}}{N}=\frac{n_B}{2}\int f_l(r)\Big[-\frac{\hbar^2}{m}\nabla^2+v(r)\Big]f_l(r)\,\mathrm{d}^3\mathbf{r}. \tag{9}$$

The idea of the LOCV method is now to introduce a healing distance $d$ beyond which the pair correlation function $f_l$ is constant,

$$f_l(r>d)=1. \tag{10}$$

To ensure that the derivative of $f_l$ is continuous at $r=d$, an additional constraint is introduced,

$$f_l'(r=d)=0. \tag{11}$$

Introducing a constant average field $\lambda_l$ and varying with respect to $f_l$ while using that $f_l$ is constant for $r>d$, gives the Schrödinger-like two-body equation for $r<d$,

$$\Big[-\frac{\hbar^2}{m}\nabla^2+v(r)\Big](rf_l(r))=\lambda_l r f_l(r). \tag{12}$$

Finally, the condition

$$n_B\int_0^d f_l^2(r)\,\mathrm{d}^3\mathbf{r}=1 \tag{13}$$

enforces that the average number of particles within $d$ equals 1. Using Eqs. (9), (10) and (12), the energy per particle becomes,

$$\frac{E_{B,l}}{N}=\frac{\lambda_l}{2}+\frac{n_B}{2}\int_d^\infty v(r)\mathrm{d}^3\mathbf{r}. \tag{14}$$

The second term on the right hand side of Eq. (14) is identically zero for the square well potential $v_{sw}$ but contributes a so-called tail or mean-field energy for the van der Waals potential $v_{vdw}$ [27, 28]. We determine the three unknown $n_B$, $\lambda_l$ and $d$ by simultaneously solving Eqs. (12) and (13) subject to the boundary condition given by Eq. (11). Note that $n_B$ and $d$ depend, just as $f_l$ and $\lambda_l$, on the angular momentum; the subscript has been dropped, however, for notational convenience.

In addition to one-component Bose systems, Sec. IV considers two-component Bose systems, characterized by $l$-wave interspecies and vanishing intraspecies interactions. The Hamiltonian for the two-component Bose system is given by Eq. (2), with the sum of the two-body interactions restricted to unlike bosons. Correspondingly, the product wave function is written as a product of pair functions, including only correlations between unlike bosons. The LOCV equations are then given by Eqs. (10) through (13) with $n_B$ in Eq. (13) replaced by $n_B/2$.

Next, we discuss how to determine the energy $E_{F,l}/N$ per particle for a two-component Fermi system within the LOCV method [29, 30, 31, 32]. The wavefunction is taken to be

$$\Psi_F(\mathbf{r}_1,\ldots,\mathbf{r}_{1'},\ldots)=\Phi_{FG}\prod_{i,j'} f_l(r_{ij'}), \tag{15}$$

where $\Phi_{FG}$ denotes the ground state wavefunction of the non-interacting Fermi gas. The product of pair functions $f_l$ accounts for the correlations between unlike fermions. In accord with our assumption that like fermions are non-interacting, Eq. (15) treats like fermion pairs as uncorrelated. Neglecting exchange effects, the derivation of the LOCV equations parallels that outlined above for the bosons. The boundary conditions, given by Eqs. (10) and (11), and the Schrödinger-like differential equation for $\lambda_l$, Eq. (12), are unchanged. The "normalization condition," however, becomes

$$\frac{n_F}{2}\int_0^d f_l^2(r)\mathrm{d}^3\mathbf{r}=1, \tag{16}$$

where the left-hand side is the number of fermion pairs within $d$. The fermion energy per particle is then the sum of the one-particle contribution from the non-interacting Fermi gas and the pair correlation energy $\lambda_l$ [20],

$$E_{F,l}/N=E_{FG}+\frac{\lambda_l}{2}. \tag{17}$$

This equation excludes the contribution from the tail of the potential, i.e., the term analogous to the second term on the right hand side of Eq. (14), since this term is negligible for the fermion densities considered in this paper.

The LOCV solutions for $f_l$, $\lambda_l$ and $d$ for the homogeneous one-component Bose system and the two-component Fermi system are formally identical if the boson density is chosen to equal half the fermion density, i.e., if $n_B=n_F/2$. This relation can be understood by realizing that any given fermion (e.g., a spin-up particle) interacts with only half of the total number of fermions (e.g., all the spin-down fermions). Consequently, the two-component Fermi system appears twice as dense as the one-component Bose system. The fact that the LOCV solutions for bosons can be converted to LOCV solutions for fermions suggests that some physics of the bosonic system can be understood in terms of the fermionic system and vice versa. In fact, it has been shown previously [20] that the LOCV energy for the first excited gas-like state of $s$-wave interacting fermions at unitarity can be derived from the LOCV energy of the energetically lowest-lying gas-like branch of $s$-wave interacting bosons [12]. Here, we extend this analysis and show that the ground state energy of the Fermi gas at unitarity can

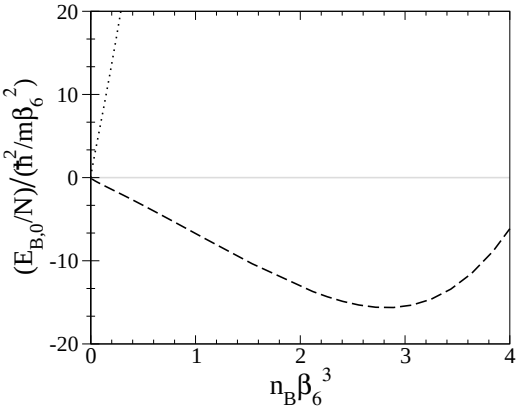


FIG. 1: Energy per particle $E_{B,0}/N$ as a function of the density $n_B$, both plotted as dimensionless quantities, for a one-component Bose system interacting through the van der Waals potential with $s$-wave scattering length $a_s = 16.9\beta_6$. The dotted line shows the gas branch and the dashed line the liquid branch. The minimum of the liquid branch is discussed in reference to liquid $^4$He in the text.

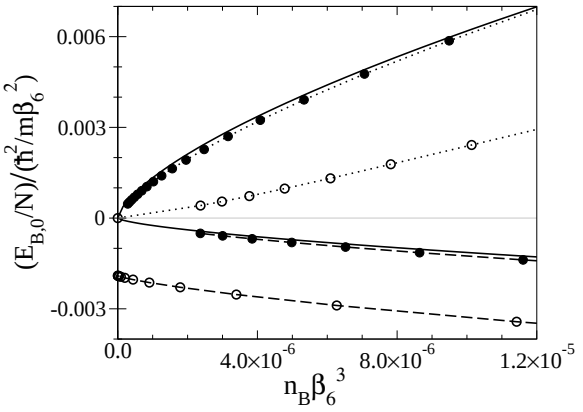


FIG. 2: Energy per particle $E_{B,0}/N$ as a function of the density $n_B$ for a one-component Bose system interacting through the van der Waals potential with $s$-wave scattering lengths $a_s = 16.9\beta_6$ (open circles) and $a_s = 169\beta_6$ (filled circles). To guide the eye, dashed and dotted lines connect the data points of the liquid and gas branches, respectively. The liquid branches go to $E_{dimer}/2$ as the density goes to zero. The solid lines show $E_{B,0}/N$ at unitarity; see text for discussion. Compared to Fig. 1, the energy and density scales are greatly enlarged.

be derived from the energetically highest-lying liquid-like branch of the Bose system. Furthermore, we extend this analysis to higher angular momentum scattering.

## III. $s$-WAVE INTERACTING BOSE AND FERMI SYSTEMS

Figure 1 shows the energy per particle $E_{B,0}/N$, Eq. (14), obtained by solving the LOCV equations for a one-component Bose system interacting through the van der Waals potential with $s$-wave scattering length $a_s = 16.9\beta_6$. The dotted line in Fig. 1 has positive energy and increases with increasing density; it describes the energetically lowest-lying "gas branch" for the Bose system with $a_s = 16.9\beta_6$ and corresponds to the metastable gaseous condensate studied experimentally. The dashed line in Fig. 1 has negative energy at small densities, decreases with increasing density, and then exhibits a minimum; this dashed line describes the energetically highest-lying "liquid branch" for a Bose system with $a_s = 16.9\beta_6$. Within the LOCV framework, these two branches arise because the Schrödinger-like equation, Eq. (12), permits for a given interaction potential solutions $f_0$ with differing number of nodes, which in turn give rise to a host of liquid and gas branches [27, 28]. Throughout this work we only consider the energetically highest-lying liquid branch with $n$ nodes and the energetically lowest-lying gas branch with $n+1$ nodes. To obtain Fig. 1, we consider a class of two-body potentials with fixed $a_s/\beta_6$, and decrease the value of the ratio $r_c/\beta_6$ till $E_{B,0}/N$, Eq. (14), no longer changes over the density range of interest, i.e., the number of nodes $n$ of the energetically highest-lying liquid branch is increased till convergence is reached.

In Fig. 1, the two-body van der Waals potential is chosen so that the scattering length of $a_s = 16.9\beta_6$ coincides with that of the $^4$He pair potential [37]. The liquid branch in Fig. 1 can hence be applied to liquid $^4$He, and has previously been considered in Refs. [27, 28]. The minimum of the liquid branch at a density of $n_B = 2.83\beta_6^{-3}$, or $1.82 \times 10^{22}\text{cm}^{-3}$, agrees quite well with the experimental value of $2.18 \times 10^{22}\text{cm}^{-3}$ [38]. The corresponding energy per particle of $-6.56$ K deviates by 8.5 % from the experimental value of $-7.17$ K [38]. This shows that the LOCV framework provides a fair description of the strongly interacting liquid $^4$He system, which is characterized by interparticle spacings comparable to the range of the potential. This is somewhat remarkable considering that the LOCV method includes only pair correlations and that the van der Waals potential used here contains only two parameters.

Open circles connected by a dashed line in Fig. 2 show the liquid branch for $a_s = 16.9\beta_6$ in the small density region. As the density goes to zero, the energy per particle $E_{B,0}/N$ does not terminate at zero but, instead, goes to $E_{dimer}/2$, where $E_{dimer}$ denotes the energy of the most weakly-bound $s$-wave molecule of $v_{vdw}$. In this small density limit, the liquid branch describes a gas of weakly-bound molecules, in which the interparticle spacing between the molecules greatly exceeds the size of the molecules, and $E_{dimer}$ is to a very good approximation given by $-\hbar^2/(ma_s^2)$. As seen in Fig. 2, we find solutions in the whole density range considered. In contrast to our findings, Ref. [28] reports that the LOCV solutions of the liquid branch disappear at densities smaller than a scattering length dependent critical density, i.e.,

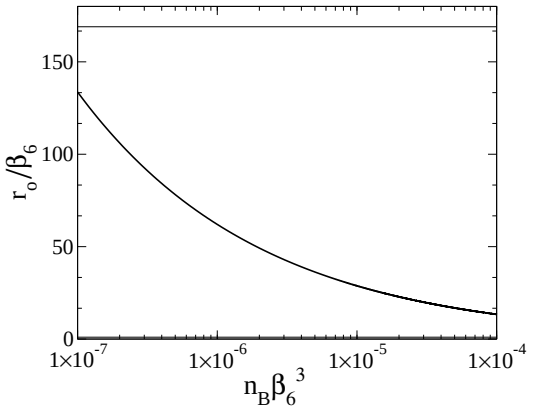


FIG. 3: Scaled interparticle spacing $r_o/\beta_6$ as a function of the scaled density $n_B\beta_6^3$ for the gas branch of a one-component Bose system interacting through the van der Waals potential with $a_s = 169\beta_6$. The horizontal lines show the scaled $s$-wave scattering length $a_s = 169\beta_6$ and the range of the van der Waals potential, which is one in scaled units (almost indistinguishable from the $x$-axis). This graph shows that the unitary inequalities $a_s \gg r_o \gg \beta_6$ hold for $n_B$ larger than about $10^{-5}\beta_6^{-3}$.

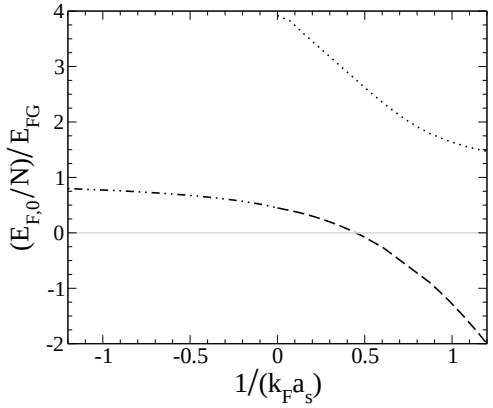


FIG. 4: Scaled energy per particle $(E_{F,0}/N)/E_{FG}$ as a function of $1/(k_Fa_s)$ for a two-component $s$-wave Fermi gas interacting through the square well potential for $n_F = 10^{-6}R^{-3}$. The combined dashed and dash-dotted curve corresponds to the BEC-BCS crossover curve and the dotted curve corresponds to the first excited state of the Fermi gas. The dashed and dotted linestyles are chosen to emphasize the connection to the gas and liquid branches of the Bose system in Figs. 2 and 3 (see text for more details).

at a critical density of $8.68 \times 10^{-7}\beta_6^{-3}$ for $a_s = 16.9\beta_6$. Thus we are not able to reproduce the liquid-gas phase diagram proposed in Fig. 2 of Ref. [28], which depends on this termination of the liquid branch. We note that the liquid branch is, as indicated by its imaginary speed of sound, dynamically unstable at sufficiently small densities. The liquid of weakly-bound bosonic molecules discussed here can, as we show below, be related to weakly-bound molecules on the BEC side of the BEC-BCS crossover curve for two-component Fermi gases.

We now discuss the gas branch in more detail. Open and filled circles connected by dotted lines in Fig. 2 show the energy per particle for $a_s = 16.9\beta_6$ and $169\beta_6$, respectively. These curves can be applied, e.g., to $^{85}$Rb, whose scattering length can be tuned by means of a Feshbach resonance and which has a $\beta_6$ value of $164a_{bohr}$, where $a_{bohr}$ denotes the Bohr radius. For this system, a scattering length of $a_s = 16.9\beta_6$ corresponds to $2770a_{bohr}$, a comparatively large value that can be realized experimentally in $^{85}$Rb gases. As a point of reference, a density of $10^{-5}\beta_6^{-3}$ corresponds to a density of $1.53 \times 10^{13}\text{cm}^{-3}$ for $^{85}$Rb.

The solid curve with positive energy in Fig. 2 shows the energy per particle $E_{B,0}/N$ at unitarity, $E_{B,0}/N \approx 13.3\hbar^2 n_B^{2/3}/m$ [12]. As seen in Fig. 2, this unitary limit is approached by the energy per particle for the Bose gas with $a_s = 169\beta_6$ (filled circles connected by a dotted line). To illustrate this point, Fig. 3 shows the scaled average interparticle spacing $r_o/\beta_6$ as a function of the scaled density $n_B\beta_6^3$ for $a_s = 169\beta_6$. This plot indicates that the unitary requirement, $a_s \gg r_o \gg R$, is met for values of $n_B\beta_6^3$ larger than about $10^{-5}$. Similarly, we find that the family of liquid curves converges to $E_{B,0}/N \approx -2.46\hbar^2 n_B^{2/3}/m$ (see Sec. IV for details), plotted as a solid line in Fig. 2, when the inequalities $a_s \gg r_o \gg \beta_6$ are fullfilled. We note that the unitarity curve with negative energy is also approached, from above, for systems with large negative scattering lengths (not shown in Fig. 2). Aside from the proportionality constant, the power law relation for the liquid and gas branches at unitarity is the same.

In addition to a Bose system interacting through the van der Waals potential, we consider a Bose system interacting through the square well potential with range $R$. For a given scattering length $a_s$ and density $n_B$, the energy per particle $E_{B,0}/N$ for these two two-body potentials is essentially identical for the densities shown in Fig. 2. This agreement emphasizes that the details of the two-body potential become negligible at low density, and in particular, that the behavior of the Bose gas in the unitary limit is governed by a single length scale, the average interparticle spacing $r_o$.

As discussed in Sec. II, the formal parallels between the LOCV method applied to bosons and fermions allows the energy per particle $E_{F,0}/N$ for a two-component Fermi gas, Eq. (17), to be obtained straightforwardly from the energy per particle $E_{B,0}/N$ of the Bose system. Figure 4 shows the dimensionless energy $(E_{F,0}/N)/E_{FG}$ as a function of the dimensionless quantity $1/(k_Fa_s)$ for the square well potential for $n_F = 10^{-6}R^{-3}$. We find essentially identical results for the van der Waals potential. The crossover curve shown in Fig. 4 describes any dilute Fermi gas for which the range $R$ of the two-body potential is very small compared to the average interparticle

spacing $r_o$. In converting the energies for the Bose system to those for the Fermi system, the gas branches of the Bose system (dotted lines in Figs. 2 and 3) "turn into" the excited state of the Fermi gas (dotted line in Fig. 4); the liquid branches of the Bose system with positive $a_s$ (dashed lines in Figs. 2 and 3) "turn into" the part of the BEC-BCS crossover curve with positive $a_s$ (dashed line in Fig. 4); and the liquid branches of the Bose system with negative $a_s$ (not shown in Figs. 2 and 3) "turn into" the part of the BEC-BCS crossover curve with negative $a_s$ (dash-dotted line in Fig. 4).

To emphasize the connection between the Bose and Fermi systems further, let us consider the BEC side of the crossover curve. If $1/(k_F a_s) \gtrsim 1$, the fermion energy per particle $E_{F,0}/N$ is approximately given by $E_{dimer}/2$, which indicates that the Fermi gas forms a molecular Bose gas. Similarly, the liquid branch of the Bose system with positive scattering length is made up of bosonic molecules as the density goes to zero. The formal analogy between the Bose and Fermi LOCV solutions also allows the energy per particle $E_{F,0}/N$ at unitarity, i.e., in the $1/(k_F|a_s|) \to 0$ limit, to be calculated from the energies for large $a_s$ of the gas and liquid branches of the Bose system (solid lines in Fig. 2). For the excited state of the Fermi gas we find $E_{F,0}/N \approx 3.92 E_{FG}$, and for the lowest gas state we find $E_{F,0}/N \approx 0.46 E_{FG}$. These results agree with the LOCV calculations of Ref. [20], which use an attractive cosh-potential and a $\delta$-function potential. The value of $0.46 E_{FG}$ is in good agreement with the energy of $0.42 E_{FG}$ obtained by fixed-node diffusion Monte Carlo calculations [21, 22].

## IV. BOSE AND FERMI SYSTEMS BEYOND $s$-WAVE AT UNITARITY

This section investigates the unitary regime of Bose and Fermi systems interacting through higher angular momentum resonances. These higher angular momentum resonances are necessarily narrow [9], and we hence expect the energy-dependence of the generalized scattering length $a_l(k)$ to be particularly important in understanding the many-body physics of dilute atomic systems beyond $s$-wave. In the following we focus on the strongly-interacting limit. Figure 5 shows $1/a_l(k)$ as a function of the relative scattering energy $E_{rel}$ for the square-well potential with infinite zero-energy scattering length $a_l$ for three different angular momenta, $l = 0$ (solid line), $l = 1$ (dashed line), and $l = 2$ (dotted line). Figure 5 shows that the energy-dependence of $a_l(k)$ increases with increasing $l$.

Our goal is to determine the energy per particle $E_{B,l}/N$ for Bose systems with finite angular momentum $l$ in the strongly-interacting regime. For $s$-wave interactions, the only relevant length scale at unitarity is the average interparticle spacing $r_o$ (see Sec. III). In this case, the energy per particle at unitarity can be estimated analytically by evaluating the LOCV equations subject to

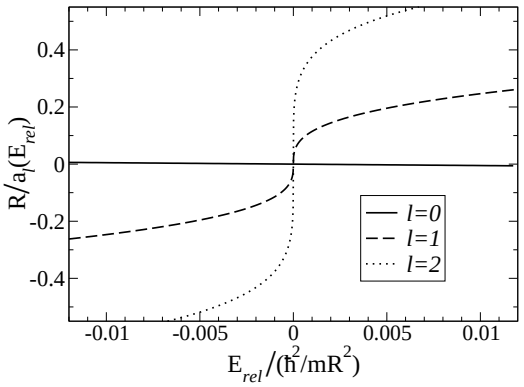


FIG. 5: $R/a_l(E_{rel})$ as a function of the scaled relative scattering energy $E_{rel}/(\hbar^2/mR^2)$ for the square well potential $v_{sw}$ with infinite zero-energy scattering length $a_l$, i.e., $1/a_l = 0$, for three different partial waves [$l = 0$ (solid line), $l = 1$ (dashed line), and $l = 2$ (dotted line)].

the boundary condition implied by the zero-range $s$-wave pseudo-potential [12]. Unfortunatey, a similarly simple analysis that uses the boundary condition implied by the two-body zero-range pseudo-potential for higher partial waves fails. This combined with the following arguments suggests that $E_{B,l}/N$ depends additionally on the range of the underlying two-body potential for finite $l$: i) The probability distribution of the two-body $l$-wave bound state, $l > 0$, remains finite as $a_l$ approaches infinity and depends on the interaction potential [39, 40]. ii) A description of $l$-wave resonances ($l > 0$) that uses a coupled channel square well model depends on the range of the square well potential [41]. iii) The calculation of structural expectation values of two-body systems with finite $l$ within a zero-range pseudo-potential treatment requires a new length scale to be introduced [26].

Motivated by these two-body arguments (see also Refs. [42, 43, 44] for a treatment of $p$-wave interacting Fermi gases) we propose the following functional form for the energy per particle $E_{B,l}/N$ of a $l$-wave Bose system at unitarity interacting through the square-well potential $v_{sw}$ with range $R$,

$$\frac{E_{B,l}}{N} = C_l \, \frac{\hbar^2}{m R^{x_l/2}} \, n_B^{2/3 - x_l/6}. \qquad (18)$$

Here, $C_l$ denotes a dimensionless $l$-dependent proportionality constant. The dimensionless parameter $x_l$ determines the powers of the range $R$ and the density $n_B$, and ensures the correct units of the right hand side of Eq. (18). To test the validity of Eq. (18), we solve the LOCV equations, Eqs. (11) through (14), for $l = 0$ to 2 for the one-component Bose system. Note that the one-component $p$-wave system is unphysical since it does not obey Bose symmetry; we nevertheless consider it here since its LOCV energy determines the energy of two-component $p$-wave Bose and Fermi systems (see below).

Figure 6 shows the energy per particle $E_{B,l}/N$ for

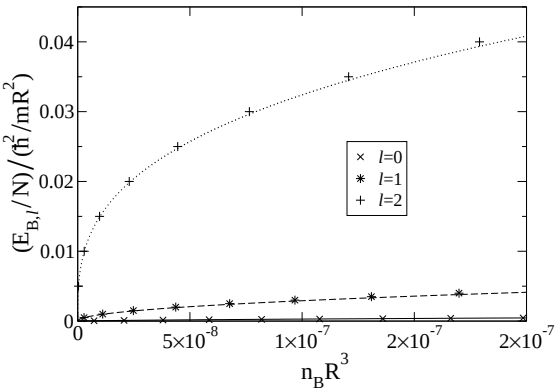


FIG. 6: Scaled energy per particle $(E_{B,l}/N)/(\hbar^2/mR^2)$ for a one-component Bose system for the energetically lowest-lying gas branch as a function of the scaled density $n_B R^3$ obtained by solving the LOCV equations [Eqs. (11) through (14)] for $v_{sw}$ for three different angular momenta $l$ [$l = 0$ (crosses), $l = 1$ (asterisks) and $l = 2$ (pluses)]. The depth $V_0$ of $v_{sw}$ is adjusted so that $1/a_l(k) = 0$. Solid, dotted and dashed lines show fits of the LOCV energies at low densities to Eq. (18) for $l = 0$, $l = 1$ and $l = 2$ (see text for details). Note that the system with $l = 1$ is of theoretical interest but does not describe a physical system.

| $l$ | $x_l$ | $C_l^L$ | $C_l^G$ |
|---|---|---|---|
| 0 | 0.00 | −2.46 | 13.3 |
| 1 | 1.00 | −3.24 | 9.22 |
| 2 | 2.00 | −3.30 | 6.98 |

TABLE I: Dimensionless parameters $x_l$, $C_l^L$ and $C_l^G$ for $l = 0$ to 2 for a one-component Bose system obtained by fitting the LOCV energies $E_{B,l}/N$ for small densities to the functional form given in Eq. (18) (see text for details).

a one-component Bose system, obtained by solving the LOCV equations for the energetically lowest-lying gas branch, as a function of the density $n_B$ for $l = 0$ (crosses), $l = 1$ (asterisks), and $l = 2$ (pluses) for the square well potential, whose depth $V_0$ is adjusted for each $l$ so that the *energy-dependent* generalized scattering length $a_l(k)$ diverges, i.e., $1/a_l(k) = 0$. Setting $a_l(k)$ to infinity ensures that the $l$-wave interacting Bose system is infinitely strongly interacting over the entire density regime shown in Fig. 6. Had we instead set the zero-energy scattering length $a_l$ to infinity, the system would, due to the strong energy-dependence of $a_l(k)$ [see Fig. 5], "effectively" interact through a finite scattering length.

Table I summarizes the values for $x_l$ and $C_l^G$, which we obtain by performing a fit of the LOCV energies $E_{B,l}/N$ for the one-component Bose system for small densities to the functional form given in Eq. (18). In particular, we find $x_l = l$, which implies that $E_{B,l}/N$ varies as $n_B^{2/3}$, $n_B^{1/2}$ and $n_B^{1/3}$ for $l = 0$, 1 and 2, respectively. Table I uses the superscript "$G$" to indicate that the proportionality constant is obtained for the energetically lowest-lying gas branch. The density ranges used in the fit are chosen so that Eq. (18) describes the low-density or universal regime accurately. Solid, dotted and dashed lines in Fig. 6 show the results of these fits for $l = 0$, 1 and 2, respectively; in the low density regime, the lines agree well with the symbols thereby validating the functional form proposed in Eq. (18).

We repeat the LOCV calculations for the energetically highest-lying liquid branch of the one-component Bose system. By fitting the LOCV energies of the liquid branches for small densities to Eq. (18), we determine $x_l$ and $C_l$ [45]. We find the same $x_l$ as for the gas branch but different $C_l$ than for the gas branch (the proportionality constants obtained for the liquid branch are denoted by $C_l^L$; see Table I). Our values for $x_0$, $C_0^G$ and $C_0^L$ agree with those reported in the literature [12, 20, 46].

Equation (18) can be rewritten in terms of the combined length $\xi_l$,

$$\frac{E_{B,l}}{N} = C_l \Big(\frac{4}{3}\pi\Big)^{(l/6-2/3)} \frac{\hbar^2}{m\xi_l^2}, \tag{19}$$

where

$$\xi_l = r_o^{(1-l/4)} R^{l/4}. \tag{20}$$

For the $s$-wave case, $\xi_l$ reduces to $r_o$ and the convergence to the unitary regime can be seen by plotting $(E_{B,0}/N)/(\hbar^2/mr_o^2)$ as a function of $a_s/r_o$ [12]. To investigate the convergence to the unitary regime for higher partial waves, Fig. 7 shows the energy per particle $E_{B,l}/N$ for the energetically lowest-lying gas branch as a function of $a_l(E_{rel})/\xi_l$ for fixed energy-dependent scattering lengths $a_l(k)$, i.e., for $a_s(k) = 10^{10}R$, $a_p(k) = 10^{10}R$, and $a_d(k) = 10^6 R$ [the different values of $a_l(k)$ are chosen for numerical reasons]. Figure 7 shows that the inequality

$$|a_l(E_{rel})| \gg \xi_l \gg R \tag{21}$$

is fulfilled when $(E_{B,l}/N)/(\hbar^2/m\xi_l^2)$ is constant. Note that this inequality is written in terms of the energy-dependent scattering length (see above). We find similar results for the liquid branches for $l = 0$ to 2. For higher partial waves, we hence use the inequality given by Eq. (21) to define the unitary regime. In the unitary regime, the energy per particle $E_{B,l}/N$ of the Bose system depends only on the combined length scale $\xi_l$. For $s$-wave interacting systems, we have $\xi_s = r_o$ and $a_s(k) \approx a_s$, and Eq. (21) reduces to the well known $s$-wave unitary condition, i.e., to $|a_s| \gg r_o \gg R$.

We now discuss those regions of Fig. 7, where the energy per particle $(E_{B,l}/N)/(\hbar^2/m\xi_l^2)$ for the one-component Bose system deviates from a constant. For sufficiently large densities, the characteristic length $\xi_l$ becomes of the order of the range $R$ of the square well potential. In this "high density" regime the system exhibits non-universal behaviors. In Fig. 7, e.g., the energy-dependent scattering length $a_d(k)$ equals $10^6 R$;

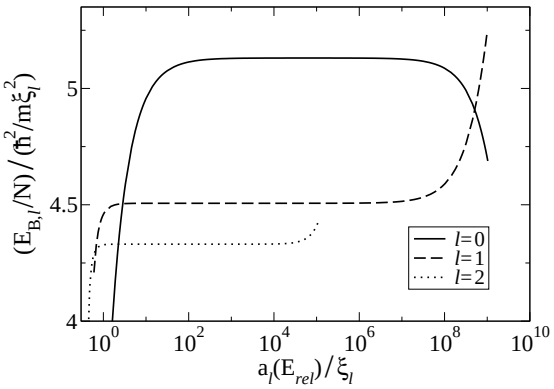


FIG. 7: Scaled energy per particle $(E_{B,l}/N)/(\hbar^2/m\xi_l^2)$ for the energetically lowest-lying gas branch of $l$-wave interacting one-component Bose systems obtained by solving the LOCV equations [Eqs. (11) through (14)] for $v_{sw}$ as a function of $a_l(E_{rel})/\xi_l$. The depth $V_0$ of $v_{sw}$ is adjusted so that $a_l(E_{rel}) = 10^{10}R$ for $l = 0$ and $l = 1$, and $a_l(E_{rel}) = 10^6 R$ for $l = 2$. Note that the system with $l = 1$ is of theoretical interest but does not describe a physical system. In the regime where the inequality $R \ll \xi_l \ll a_l(E_{rel})$ is fulfilled, the scaled energy per particle is constant; this defines the unitary regime.

correspondingly, $\xi_d$ equals $R$ when $a_d(k)/\xi_d = 10^6$. As $a_d(k)/\xi_d$ approaches $10^6$ from below, the system becomes non-universal, as indicated in Fig. 7 by the non-constant dependence of the scaled energy per particle on $a_d(k)/\xi_d$. On the left side of Fig. 7, where $a_l(E_{rel})/\xi_l$ becomes of order 1, the "low density" end of the unitary regime is reached. When $a_p(E_{rel})/\xi_p$ equals 10, e.g., the interparticle spacing $r_o$ equals $10^2 a_p(E_{rel})$, i.e., the system exhibits universal behavior even when the interparticle spacing is 100 times larger than the scattering length $a_p(E_{rel})$. This is in contrast to the $s$-wave case, where the universal regime requires $|a_s| \gg r_o$. The different behavior of the higher partial wave systems compared to the $s$-wave system can be understood by realizing that $\xi_l$ is a combined length, which contains both the range $R$ of the two-body potential and the average interparticle spacing $r_o$. For a given $a_l(E_{rel})/R$, the first inequality in Eq. (21) is thus satisfied for larger average interparticle spacings $r_o/R$, or smaller scaled densities $n_B R^3$, as $l$ increases from 0 to 2.

In addition to investigating $l$-wave Bose gases interacting through the square well potential $v_{sw}$, we consider the van der Waals potential $v_{vdw}$. For the energetically lowest-lying gas branch of the one-component "$p$-wave Bose" system we find the same results as for the square well potential if we replace $R$ in Eqs. (18) to (20) by $\beta_6$. We believe that the same replacement needs to be done for the liquid branch with $l = 1$ and for the liquid and gas branches of $d$-wave interacting bosons, and that the scaling at unitarity derived above for the square well potential holds for a wide class of two-body potentials.

Within the LOCV framework, the results obtained for

| $l$ | $x_l$ | $C_l^L$ | $C_l^G$ |
|---|---|---|---|
| 0 | 0.00 | −1.55 | 8.40 |
| 1 | 1.00 | −2.29 | 6.52 |
| 2 | 2.00 | −2.62 | 5.54 |

TABLE II: Dimensionless parameters $x_l$, $C_l^L$ and $C_l^G$ for $l = 0$ to 2 for a two-component Bose system (see text for details).

$x_l$, $C_l^G$ and $C_l^L$ for the one-component Bose systems can be applied readily to the corresponding two-component system by scaling the Bose density appropriately (see Sec. II). The resulting parameters $x_l$, $C_l^L$ and $C_l^G$ for the two-component Bose systems are summarized in Table II.

The energy per particle $E_{F,l}/N$ for $l$-wave interacting two-component Fermi systems can be obtained from Eq. (17) using the LOCV solutions for the liquid and gas branches discussed above for $l$-wave interacting one-component Bose systems. In the unitary limit, we find

$$\frac{E_{F,l}}{N} = A\frac{\hbar^2}{m}n_F^{2/3} + B_l\frac{\hbar^2}{m}\frac{n_F^{2/3-l/6}}{R^{l/2}}, \qquad (22)$$

where $A = (3/10)(3\pi^2)^{2/3} \approx 2.87$ and $B_l = C_l^{G,L}/2^{2/3-l/6}$ (the $C_l^{G,L}$ are given in Table I). The first term on the right hand side of Eq. (22) equals $E_{FG}$, and the second term, which is obtained from the LOCV solutions, equals $\lambda_l/2$. The energy per particle $E_{F,l}/N$ at unitarity is positive for all densities for $B_l = C_l^G/2^{2/3-l/6}$. For $B_l = C_l^L/2^{2/3-l/6}$, however, the energy per particle $E_{F,l}/N$ at unitarity is negative for $l > 0$ for small densities, and goes through a minimum for larger densities. This implies that this branch is always mechanically unstable in the dilute limit for $l > 0$.

The LOCV treatment for fermions relies heavily on the product representation of the many-body wave function, Eq. (15), which in turn gives rise to the two terms on the right hand side of Eq. (22). It is the competition of these two energy terms that leads to the energy minimum discussed in the previous paragraph. Future work needs to investigate whether the dependence of $E_{F,l}/N$ on two length scales as implied by Eq. (22) is correct. In contrast to the LOCV method, mean-field treatments predict that the energy at unitarity is proportional to $E_{FG}|k_F r_{e,l}|$, where $r_{e,l}$ denotes a range parameter that characterizes the underlying two-body potential [42, 43, 44].

## V. CONCLUSION

This paper investigates Bose and Fermi systems using the LOCV method, which assumes that three- and higher-order correlations can be neglected and that the behaviors of the many-body system are governed by two-body correlations. This assumption allows the many-body problem to be reduced to an effective two-body problem. Besides the reduced numerical effort, this formalism allows certain aspects of the many-body physics

to be interpreted from a two-body point of view. Furthermore, it allows parallels between Bose and Fermi systems to be drawn.

In agreement with previous studies, we find that the energy per particle "corrected" by the dimer binding energy, i.e., $E_{F,0}/N - E_{dimer}/2$, of dilute two-component $s$-wave Fermi gases in the whole crossover regime depends only on the $s$-wave scattering length and not on the details of the underlying two-body potential. Furthermore, at unitarity the energy per particle is given by $E_{F,0}/N = 0.46E_{FG}$. This LOCV result is in good agreement with the energy per particle obtained from fixed-node diffusion Monte Carlo calculations, which predict $E_{F,0}/N = 0.42E_{FG}$ [19, 20, 21]. This agreement may be partially due to the cancellation of higher-order correlations, and thus somewhat fortuitous. In contrast to Ref. [28], we find that the liquid branch of bosonic helium does not terminate at low densities but exists down to zero density.

For higher angular momentum interactions, we determine the energy per particle of one- and two-component Bose systems with infinitely large scattering lengths. For these systems, we expect the LOCV formalism to predict the dimensionless exponent $x_l$, which determines the functional dependenc of $E_{B,l}/N$ on the range $R$ of the two-body potential and on the average interparticle spacing $r_o$, correctly. The values of the proportionality constants $C_l^G$ and $C_l^L$, in contrast, may be less accurate. We use the LOCV energies to generalize the known unitary condition for $s$-wave interacting systems to systems with finite angular momentum. Since higher angular momentum resonances are necessarily narrow, leading to a strong energy-dependence of the scattering strength, we define the universal regime using the energy-dependent scattering length $a_l(k)$. In the unitary regime, the energy per particle can be written in terms of the length $\xi_l$, which is given by a geometric combination of $r_o$ and $R$. The LOCV framework also allows a prediction for the energy per particle of two-component Fermi gases beyond $s$-wave to be made [see Eq. (22)]. Although the functional form of the many-body wave function for two-component Fermi systems used in this work may not be the best choice, we speculate that the energy scales derived for strongly interacting Bose systems are also relevant to Fermi systems.

This work was supported by the NSF through grant PHY-0555316. RMK gratefully acknowledges hospitality of the BEC Center, Trento.


[1] W. C. Stwalley, Phys. Rev. Lett. **37**, 1628 (1976).
[2] E. Tiesinga, B. J. Verhaar, and H. T. C. Stoof, Phys. Rev. A **47**, 4114 (1993).
[3] S. Inouye, M. R. Andrews, J. Stenger, H. J. Miesner, D. M. Stamper-Kurn, and W. Ketterle, Nature **392**, 151 (1998).
[4] P. Courteille, R. S. Freeland, D. J. Heinzen, F. A. van Abeelen, and B. J. Verhaar, Phys. Rev. Lett. **81**, 69 (1998).
[5] C. A. Regal, C. Ticknor, J. L. Bohn, and D. S. Jin, Phys. Rev. Lett. **90**, 053201 (2003).
[6] J. Zhang, E. G. M. van Kempen, T. Bourdel, L. Khaykovich, J. Cubizolles, F. Chevy, M. Teichmann, L. Tarruell, S. J. J. M. F. Kokkelmans, and C. Salomon, Phys. Rev. A **70**, 030702(R) (2004).
[7] C. Chin, V. Vuletić, A. J. Kerman, and S. Chu, Phys. Rev. Lett. **85**, 2717 (2000).
[8] T. Köhler, K. Góral, and P. S. Julienne, Rev. Mod. Phys. **78**, 1311 (2006).
[9] L. D. Landau and E. M. Lifshitz, *Quantum Mechanics (Non-relativistic theory), Vol. 3, 3rd Edition* (Butterworth Heinemann, Oxford, 1977).
[10] G. A. Baker, Jr., Phys. Rev. C **60**, 054311 (1999).
[11] H. Heiselberg, Phys. Rev. A **63**, 043606 (2001).
[12] S. Cowell, H. Heiselberg, I. E. Mazets, J. Morales, V. R. Pandharipande, and C. J. Pethick, Phys. Rev. Lett. **88**, 210403 (2002).
[13] P. O. Fedichev, M. W. Reynolds, and G. V. Shlyapnikov, Phys. Rev. Lett. **77**, 2921 (1996).
[14] B. D. Esry, C. H. Greene, and J. P. Burke Jr., Phys. Rev. Lett. **83**, 1751 (1999).
[15] E. Nielsen and J. H. Macek, Phys. Rev. Lett. **83**, 1566 (1999).
[16] P. F. Bedaque, E. Braaten, and H.-W. Hammer, Phys. Rev. Lett. **85**, 908 (2000).
[17] K. M. O'Hara, S. L. Hemmer, M. E. Gehm, S. R. Granade, and J. E. Thomas, Science **298**, 2179 (2002).
[18] T. Bourdel, J. Cubizolles, L. Khaykovich, K. M. F. Magalhaes, S. J. J. M. F. Kokkelmans, G. V. Shlyapnikov, and C. Salomon, Phys. Rev. Lett. **91**, 020402 (2003).
[19] J. Carlson, S. Y. Chang, V. R. Pandharipande, and K. E. Schmidt, Phys. Rev. Lett. **91**, 050401 (2003).
[20] S. Y. Chang, V. R. Pandharipande, J. Carlson, and K. E. Schmidt, Phys. Rev. A **70**, 043602 (2004).
[21] G. E. Astrakharchik, J. Boronat, J. D. Casulleras, and S. Giorgini, Phys. Rev. Lett. **93**, 200404 (2004).
[22] J. Carlson and S. Reddy, Phys. Rev. Lett. **95**, 060401 (2005).
[23] For finite $l$, the term "unitary regime" refers to the regime in which the observables of the many-body system depend, as discussed in Sec. IV, in a simple way on two length scales. Since the observables in this regime depend on two length scales, the system does not, strictly speaking, exhibit universality. However, because of the rather simple dependence on these two length scales, we nevertheless use the term "universal" to refer to this regime.
[24] D. Blume and C. H. Greene, Phys. Rev. A **65**, 043613 (2002).
[25] E. L. Bolda, E. Tiesinga, and P. S. Julienne, Phys. Rev. A **66**, 013403 (2002).
[26] R. Stock, A. Silberfarb, E. L. Bolda, and I. H. Deutsch, Phys. Rev. Lett. **94**, 023202 (2005).
[27] B. Gao, J. Phys. B **37**, L227 (2004).
[28] B. Gao, Phys. Rev. Lett. **95**, 240403 (2005).
[29] V. R. Pandharipande, Nucl. Phys. **A178**, 123 (1971).
[30] V. R. Pandharipande, Nucl. Phys. **A174**, 641 (1971).

[31] V. R. Pandharipande and H. A. Bethe, Phys. Rev. C **7**, 1312 (1973).
[32] V. R. Pandharipande and K. E. Schmidt, Phys. Rev. A **15**, 2486 (1977).
[33] B. Gao, Phys. Rev. A **58**, 1728 (1998).
[34] N. F. Mott and H. S. W. Massey, *The Theory of Atomic Collisions, Third Edition* (Clarendon, Oxford, 1965).
[35] J. R. Taylor, *Scattering Theory* (Wiley, New York, 1972).
[36] The total wave function of the Bose system has to be symmetric with respect to the exchange of any two particles, which restricts the angular momentum $l$ to even values.
[37] A. R. Janzen and R. A. Aziz, J. Chem. Phys. **103**, 9626 (1995).
[38] R. De Bruyn Ouboter and C. N. Yang, Physica B **144**, 127 (1987).
[39] K. Riisager, A. S. Jensen, and P. Møller, Nuc. Phys. A **548**, 393 (1992).
[40] A. S. Jensen, K. Riisager, D. V. Fedorov, and E. Garrido, Rev. Mod. Phys. **76**, 215 (2004).
[41] C. H. Greene, unpublished notes.
[42] T.-L. Ho and R. B. Diener, Phys. Rev. Lett. **94**, 090402 (2005).
[43] C.-H. Cheng and S.-Y. Yip, Phys. Rev. Lett. **95**, 070404 (2005).
[44] M. Iskin and C. A. R. Sá de Melo, Phys. Rev. Lett. **96**, 040402 (2006).
[45] For the liquid $l = 1$ branch we do not find solutions that obey the boundary condition given by Eq. (11). Instead, we determine the healing distance $d$ by looking for the minimum of $f_1'$. We find that the value of $f_1'$ at the minimum is much smaller than the value of $f_1'$ at small $r$.
[46] Within the LOCV formalism, the value of $-2.46$ for $C_0^L$ can, as discussed in Secs. II and III, be straightforwardly converted to obtain the energy per particle $E_{F,0}/N$ of the ground state of $s$-wave interacting two-component Fermi gases at unitarity, $E_{F,0}/N = 0.46E_{FG}$ [20]. Similarly, the value of 13.3 for $C_0^G$ can be straightforwardly converted to obtain the energy per particle $E_{F,0}/N$ of the first excited gas state of $s$-wave interacting two-component Fermi gases at unitarity, $E_{F,0}/N = 3.92E_{FG}$.